ACS APPLIED MATERIALS & INTERFACES

Research Article

www.acsami.org

Hybrid Paclitaxel and Gold Nanorod-Loaded Human Serum Albumin Nanoparticles for Simultaneous Chemotherapeutic and Photothermal Therapy on 4T1 Breast Cancer Cells

Donna V. Peralta,[†] Zahra Heidari,[‡] Srikanta Dash,[§] and Matthew A. Tarr*[,†]

[†]Department of Chemistry and Advanced Materials Research Institute, University of New Orleans, New Orleans, Louisiana 70148, United States

[‡]Department of Chemical & Biomolecular Engineering, Tulane University, New Orleans, Louisiana 70118, United States

[§]Department of Pathology and Laboratory Medicine, Tulane University Health Sciences Center, New Orleans, Louisiana 70112, United States

Supporting Information

ABSTRACT: The use of human serum albumin nanoparticles (HSAPs) as a drug carrier system for cancer treatment has proven successful through current marketable clinical formulations. Despite this success, there is a current lack of multifunctional HSAPs, which offer combinational therapies of more than one proven technique. Gold nanorods (AuNRs) have also shown medicinal promise due to their photothermal therapy capabilities. In this study, a desolvation and cross-linking approach was employed to successfully encapsulate gold nanorods into HSAPs simultaneously with the chemotherapeutic drug paclitaxel (PAC); forming PAC-AuNR-HSAPs with desirable overall particle sizes of 299 ± 6 nm. The loading efficiency of paclitaxel into PAC-AuNR-HSAPs reached up to 3 μg PAC/mg HSA. The PAC-AuNR-HSAPs experienced photothermal heating; with the bulk particle solution reaching up to 46 °C after 15 min of near-IR laser exposure. This heat increase marked the successful attainment of the temperature necessary to cause severe cellular hyperthermia and necrosis. The encasement strategy facilitated a colloidal hybrid treatment system capable of enhanced permeability and retention effects, photothermal ablation of cancer cells, and release of the active paclitaxel of up to 188 ng (from PAC-AuNR-HSAPs created with 30 mg HSA) in a single 15 min irradiation session. When treated with PAC-AuNR-HSAPs containing 20 μg PAC/mL particle solution, 4T1 mouse breast cancer cells experienced ∼82% cell death without irradiation and ∼94% cell death after just one irradiation session. The results for PAC-AuNR-HSAPs were better than that of free PAC, which only killed ∼77% of the cells without irradiation and ∼80% with irradiation. The hybrid particle system also lends itself to future customizable external functionalities via conjugated targeting ligands, such as antibodies. Internal entrapment of patient tailored medication combinations are also possible with this combination treatment platform, which may result in improved quality of life for those undergoing treatment.

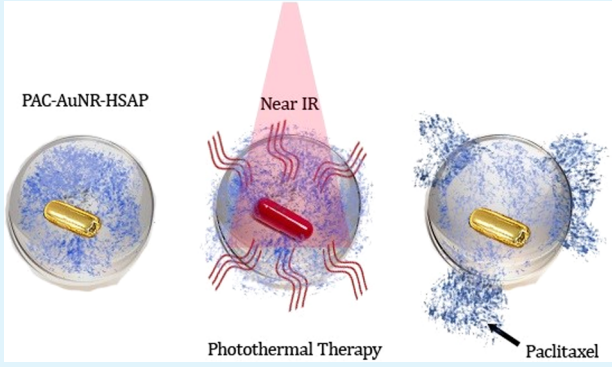

KEYWORDS: *drug delivery, photothermal therapy, hybrid nanoparticles, breast cancer, chemotherapy, biomaterials*

1. INTRODUCTION

There is a current need for multifunctional, temporally active cancer treatments, which maximize therapeutic effects through less invasive techniques. A hybridization of effective treatments can offer combinational therapy, which may result in higher success rates and increased quality of life for patients suffering with the disease. Gold nanorods (AuNRs) have the ability to absorb relatively harmless near-infrared light, causing the subsequent release of energy via heat, which can be harnessed for use in plasmonic photothermal therapy (PPTT).[1−6] Moderate cell hyperthermia occurs at 43 °C and can cause increases in endocytosis and blood flow, resulting in not only an increase in uptake of drugs, but a breakdown in cellular structure.[7] Increasing the induced temperature to over 46 °C will cause severe hyperthermia and eventual cell death through heat ablation.[8] This dose-controllable heat therapy shows immediate anticancer effects; however, the full benefits are hindered because of the distribution of energy within the beam and the gradual reduction of heat in the tissues farther from the AuNR.[9] Therefore, developing a hybrid mechanism to also carry a proven chemotherapeutic drug along with the AuNRs, with long-lasting staying power is desirable.

In a previous study, we focused on a proof-of-concept synthesis to fully encapsulate gold nanorods into HSAP spheres

Received: August 18, 2014
Accepted: March 13, 2015
Published: March 13, 2015

DOI: 10.1021/acsami.5b00858
ACS Appl. Mater. Interfaces 2015, 7, 7101−7111

to harness their PPTT effects; with the goal of keeping them from being susceptible to clearing the body as fast as smaller, drug-conjugated AuNRs prepared by other researchers.[10,11] Human serum albumin (HSA), the most abundant human blood protein, offers biocompatibility, biodegradability, and the ability to conjugate drugs and other organic and inorganic substances via covalent and noncovalent attachment to its many functional groups.[12,13] When aggregated together via a desolvation and cross-linking technique, HSA forms nanoparticles (HSAPs). These HSAPs have previously been surface modified for diagnostic and targeting functions and utilized in controlled release studies, due to enhanced permeability and retention effects (EPR); where particles of certain sizes accumulate at tumor sites.[14−16] Our previous approach allowed for internal binding to the HSA hydrophobic pockets as well as external surface functionalizing of the HSAPs, even with AuNRs present. The HSAPs are largely capable of binding a multitude of biomarkers, fluorophores, antibodies, etc.; having more binding capabilities than bare AuNRs alone.[14,17−19]

Paclitaxel (PAC) is a natural chemotherapeutic agent isolated from the bark of the western yew. PAC has been established as having major effectiveness in the treatment of metastatic breast cancer; however, it is dose limited because it has low water solubility and can cause neurotoxicity and myelosuppression among other complications.[20−22] Paclitaxel has been proven to be effective on the 4T1 mammary carcinoma breast cancer cell line; a highly invasive form of breast cancer that has been known to spontaneously metastasize.

Paclitaxel-filled HSAPs have been proven as safe medical transporters as used in the clinical formulation Abraxane, which has been successful in the treatment of lung, ovarian, breast, head and neck cancer.[23] With the FDA approval of Abraxane, paclitaxel can be used at the most antitumor efficient doses without introducing further toxicity to the patient.[21] In 2013, Abraxane was also approved for use in treating pancreatic cancer as a less toxic alternative to folfirinox and it is expected to become the standard of care for pancreatic cancer.[24−26]

The "nab-paclitaxel" particles (nanoparticle albumin-bound) allow for transport of toxic or low solubility drugs with high loading efficiency, good storage competence, and minor leakage.[27,28] Our approach utilizes this up-and-coming particle formulation and improves its treatment potential with the option of controlled heating: at lower induced temperatures, drug uptake can be facilitated and at higher induced temperature, complete cancer cell ablation is possible.[29]

The goal of this study was to substantiate the theory that proven anticancer drugs, such as PAC, could also be effectively housed within the AuNR-HSAPs, with efficient loading and that the combinatory effects of the chemotherapeutic drug and the photothermally active component could produce increased cancer cell death in the 4T1 mouse breast cancer cell line in vitro. Subsequently, proving adequate PAC release via the PPTT heating of the hybrid particles was also necessary for immediate additive treatment effects. This research supplies evidence that the PAC-AuNR-HSAP hybrid delivery system offers simultaneous drug-release and PPTT that out-performs the current free-drug, free-AuNR and PAC-HSAP platforms in vitro, while allowing for extended, controlled further release of the drug over time. The PAC-AuNR-HSAPs have the potential to be irradiated in the biologically safe water window (700−900 nm) in vivo at a tumor site up to 10 cm below the skin without affecting surrounding healthy cells, so the in vitro work represented here is a good representation of the in vivo possibilities.[9,30,31] This work shows drug-Au-HSAP hybrid composites with overall diameters of 299 ± 6 nm, which have a conceivable future as flexible, multimodal platforms for the targeted detection, contrast imaging, and selective treatment of cancer and other diseases.[32,33]

2. MATERIALS AND METHODS

2.1. Materials. Human serum albumin, lyophilized powder ≥97%, potassium bromide, Acrodisc syringe filters with nylon membrane (diameter 13 mm, pore size 0.2 μm), Corning Costar cell culture plates (flat bottom, 12 well), and 8% aqueous glutaraldehyde were obtained from Sigma-Aldrich (St. Louis, MO). Ethanol (200-proof, ACS/USP grade) was obtained from Pharmco-AAPER (CT, USA). Water was distilled, deionized, and then further purified with a Barnstead Nanopure system. Dulbecco's modified Eagle's medium (DMEM) supplemented with 5% fetal bovine serum, sodium pyruvate, nonessential amino acids, and 1% penicillin-streptomycin was obtained from Invitrogen (Carlsbad, CA).

Bare gold nanorods (10 nm average axial diameter, 43 nm average length, surface plasmon resonance ~808−829 nm, OD = 1, 5.9×10^{11} AuNR/mL in water) were obtained from Nanopartz, Inc. (Loveland, CO). The AuNRs used were advertised by the vendor as bare, but they did contain trace amounts of cetyltrimethylammonium bromide (CTAB).

The 4T1 mouse breast cancer cell line was obtained from Dr. Fred Miller at the Karmanos Cancer Institute (Detroit, MI). The 3-(4,5-dimethylthiazol-2-yl)-2,5-diphenyltetrazolium bromide, PBS buffer, Acridine Orange HCl, and anhydrous isopropanol (containing 10% Trition X-100, in 0.1 N HCl) were obtained from Sigma-Aldrich (St. Louis, Missouri, USA). The DU-530 UV/vis Life Science spectrophotometer was obtained from Beckman Coulter (Brea, CA)

2.2. Synthesis of PAC-AuNR-HSAPs, PAC-HSAPs, AuNR-HSAPs, and HSAPs. The PAC-AuNR-HSAPs were prepared using a previously devised conventional desolvation technique with the addition of AuNR seeding and drug loading, replacing pure ethanol with a PAC/ethanol solution.[11,34−36] The standard method for preparation included creating an aqueous HSA stock solution (100 mg/mL). After dissolution, the pH was around 7. To a portion of the HSA stock solution, an aliquot of the AuNR stock solution was added, along with a small stir bar. From a paclitaxel stock solution (1 mg PAC/mL ethanol), an aliquot was added dropwise to the AuNR/HSA solution flask at a rate of 1 mL/min using a peristaltic pump. Then, additional ethanol was added to achieve a final solution containing 60% ethanol. Upon the addition of the ethanol, the solution became turbid. Finally, an aliquot of 8% glutaraldehyde (aq.) was added to cross-link the PAC-AuNR-HSAPs. After the mixture was stirred for 24 h, the particles were centrifuged at 13 000 rpm (16 060*g*) for 20 min. The supernatant was removed, filtered using a 0.2 μm syringe filter, and saved for HPLC analysis. The remaining particle pellet was resuspended in a wash solution of 2:3 water/ethanol via ultrasonication. The particles were washed twice using 2:3 water/ethanol, and the supernatants were saved for HPLC analysis. The washed particles were stored at 4 °C in water. The PAC-HSAPs were created by the same process as the PAC-AuNR-HSAPs, with an aliquot of pure water substituted for the AuNR stock solution. AuNR-HSAPs also followed the same preparation parameters, with extra ethanol replacing the aliquot of paclitaxel solution. Unloaded HSAPs were formed using only water, ethanol, and 8% glutaraldehyde (aq.).

2.3. HPLC. The HPLC system used to analyze the paclitaxel was an Agilent 1100 instrument (Palo Alto, CA) with a diode array absorbance detector. The column was an Agilent Eclipse XDB-C18 column (150 × 4.6 mm, particle size 5 μm). The injection volume was 100 μL, and the wavelength used for quantitation was 227 nm. The solvent mobile phase was 45% acetonitrile and 55% water at a flow rate of 1 mL/min. The elution time for the PAC was approximately 3.8 min. Total entrapment of the drug was determined as the total mass of drug added to the particles minus the combined mass of drug in the supernatant and washes.

DOI: 10.1021/acsami.5b00858
ACS Appl. Mater. Interfaces 2015, 7, 7101−7111

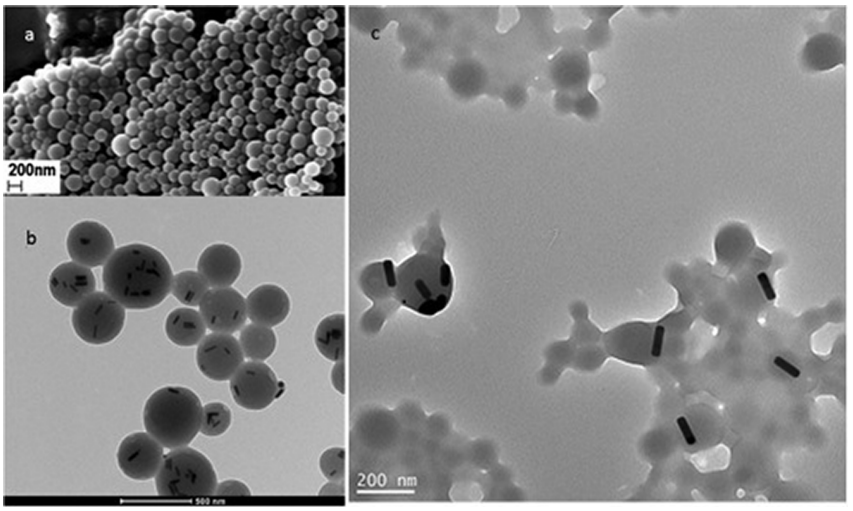

Figure 1. (a) AuNR-HSAPs visualized via FESEM image. (b) TEM image showing increased loading of AuNRs possible with 2 mg of HSA and 2 mL of AuNR stock solution. (c) TEM image of particles used in the in vitro cell studies (created with 30 mg of HSAPs and 1.5 mL of AuNR solution). Some melding of the particles caused by the electron beam is visible.

2.4. Dynamic Light Scattering. The HSAPs were characterized by measuring their diameter, mobility, and zeta potential using a Mobius dynamic light scattering (DLS) instrument (Wyatt Technology Corporation, Santa Barbara, CA). Samples were diluted with water prior to analysis.

2.5. Laser Irradiation of Particles. The PAC-AuNR-HSAPs and PAC-HSAPs were tested for heating ability and drug release under laser irradiation. To heat the samples, 1 mL of the sample was placed into a well of a 12-well plate. The plate was placed approximately 4 in. under a vertically mounted laser. A LabSpec 808 nm collimated diode laser system was used at a continuous wave power output of 2000 mW for 15, 30, or 60 min for each sample. The size of the beam was approximately 1 × 1 cm. Temperature changes caused by the irradiation sessions were measured using a Spark Science Learning System model PS-2008A thermocouple.

After irradiation, the contents of the wells were collected and centrifuged at 13 000 rpm for 15 min. The resulting supernatant was collected, diluted with ethanol, filtered, and saved for HPLC analysis.

2.6. SEM and TEM. Particles were imaged using a field emission-scanning electron microscope FESEM, LEO 1530VP (LEO Elektronenmikroskopie GmbH, Oberkochen, Germany). HSAPs were sputtered with a thin film of gold or silver to facilitate imaging. Transmission electron microscope (TEM) images were acquired with a JEOL Model 2010 TEM.

2.7. In Vitro 4T1 Breast Cancer Cells Treatment Studies. *2.7.1. MTT Assay.* The 4T1 cells (breast cancer) were cultured in high-glucose DMEM at 37 °C in a humidified atmosphere with 5% CO_2. The cells were seeded at a density of 1×10^6 cells per well into 24-well plates in triplicate. After 24 h incubation, to examine the potency of combination treatment, the cells were exposed to the following treatments: (1) PAC (ethanol as solvent), (2) HSAPs, (3) HSAPs plus laser irradiation, (4) PAC-HSAPs, (5) PAC-HSAPs plus laser irradiation, (6) AuNRs, (7) AuNRs plus laser irradiation, (8) AuNR-HSAPs, (9) AuNR-HSAPs plus laser irradiation, (10) PAC-AuNR-HSAPs, (11) PAC-AuNR-HSAPs plus laser irradiation, (12) laser irradiation, and (13) control. PAC or an equivalent concentration of PAC-AuNR-HSAP and PAC-HSAP were added at various final concentrations of 30, 20, or 10 μg/mL and were incubated for 24 h. When changing the volume of the treatment solution to manipulate paclitaxel concentration, the concentration of AuNRs in the solution was also changed, if present in the treatment formulation. The 15 min laser irradiation treatment with NIR light (λ = 808 nm; power intensity = 2 W/cm^2) was conducted 2−3 min after addition of the treatment option. Cell viability was determined using an MTT assay.

After 24 h, 1 mL of MTT solution (5 mg/mL in PBS) was added and cells were incubated for 3 h. Wells were then washed with PBS buffer (10 mM, pH 7.4) and 1 mL of anhydrous isopropanol (containing 10% Trition X-100, in 0.1 N HCl) was added and the converted dye absorbance was measured in a spectrophotometer at λ = 570 nm. The relative cell viability was proportional to the absorbance and the untreated cell control was used to approximate to 100% cells viability calculated using equation below.

$$\text{absorbance of sample/absorbance of control} \times 100\%$$

A very simple estimate (Supporting Information, Table S1) of IC_{50} values for each treatment were determined via a linear regression using the three dose concentrations of PAC (10, 20, and 30 μg/mL) and AuNRs (9.5×10^{11}, 1.92×10^{11}, and 2.88×10^{11}).

2.7.2. Microscopy Imaging of 4T1 Breast Cancer Cells. The 4T1 cells were seeded in each well of 12-well plates at a density of 1×10^6 cells/well and incubated for 24 h for cell attachment. To examine the potency of the combination treatment, the cells were exposed to the following treatments: (1) PAC (20 μg/mL in ethanol), (2) HSAPs, (3) HSAPs plus laser irradiation, (4) PAC-HSAPs (20 μg/mL PAC loaded), (5) PAC-HSAPs (20 μg/mL PAC loaded) plus laser irradiation, (6) AuNRs (1.92×10^{11} AuNRs/mL), (7) AuNRs (1.92×10^{11} AuNRs/mL) plus laser irradiation, (8) AuNR-HSAPs (1.92×10^{11} AuNRs/mL), (9) AuNR-HSAPs (1.92×10^{11} AuNRs/mL) plus laser irradiation, (10) PAC-AuNR-HSAPs (20 μg/mL PAC loaded, 1.92×10^{11} AuNRs/mL), (11) PAC-AuNR-HSAPs (20 μg/mL PAC loaded, 1.92×10^{11} AuNRs/mL) plus laser irradiation, (12) laser irradiation, and (13) control.

For the photothermal therapy studies, light was applied to the central part of the cell layer using an 808 nm CW laser (2 W/cm^2 for 15 min). Then, the cells were incubated for 24 h. Acridine Orange staining was used as an indicator in viability and cytotoxicity tests. After 24 h, the cells were washed twice with PBS buffer and stained in DMEM containing 5 mg/mL Acridine Orange for 15 min. The cells were washed three times in PBS and examined by fluorescence microscopy. The cells were monitored under an Olympus IX70 microscope (10× objective lens) and a DP-71 digital camera (Olympus, PA). Fluorescence images were taken from central areas in each case and the exposure time was 200 ms. The manufacturer's cell imaging software was used for the acquisition of microscopic images. All the data were acquired using identical settings on the microscope to ensure reproducibility.

2.8. Statistical Analysis. Cytotoxicity experiments were done with three independent replications, and all results were expressed as mean ± SD (standard deviation). Comparison between two groups was performed with a Student's t test. P-value for statistical analysis was significant when $p < 0.05$.

DOI: 10.1021/acsami.5b00858
ACS Appl. Mater. Interfaces 2015, 7, 7101−7111

3. RESULTS AND DISCUSSION

3.1. Formation of PAC-HSAPs and PAC-AuNR-HSAPs. Desolvation is a simple, thermodynamically driven self-assembly process for polymeric materials by the addition of a denaturing agent, which coacervates the polypeptide molecules in the aqueous phase, thus facilitating electrostatic and hydrophobic interactions.[37] DLS confirmed that the average particle sizes for PAC-HSAPs with no AuNRs inside (using 30 mg HSA) was 158 ± 7 nm and PAC-AuNR-HSAPs were 331 ± 3, 299 ± 6, and 212 ± 28 nm, when starting the preparation process with either 20, 30, or 50 mg HSA, respectively (while all other preparation parameters were held constant). When AuNRs were present, the overall average HSAP size increased, likely because of the AuNRs acting as seeds, taking up internal space in the HSAP, thus facilitating more HSA available for continued particle growth.

Figure 1 provides representative SEM and TEM images of the AuNR-HSAPs. Figure 1a is an SEM image of AuNR-HSAPs created for the in vitro studies. Figure 1b shows more heavily AuNR loaded particles created with less HSA (2 mg of HSA and 2 mL of AuNR stock solution) and Figure 1c shows more sparsely loaded particles created for the in vitro studies (30 mg of HSA and 1.5 mL of AuNR stock solution). Particles represented in Figure 1c were chosen for the heating and cell studies because the added HSA increased the volume capable of housing paclitaxel and allows for more controllable particle sizes. Despite the sparse gold loading present when using 30 mg of HSA and 1.5 mL of AuNR, the particles experienced heating sufficient to cause cell hyperthermia. There is a complex, nonlinear relationship between the protein:gold ratio and the observed particle size, as well as polydispersity.[11] Generally, the number of gold particles per albumin particle decreased as the protein:gold ratio increased. However, at high protein:gold ratios, many small HSAPs without gold were formed because of insufficient numbers of gold seed particles, resulting in smaller albumin particles seeded without gold.

The zeta potential (ζ, the electrokinetic potential of a molecule on its outer layer, slipping plane or diffuse layer), gives insight into the charge and stability of the HSAPs as a colloid.[38] As a rule of thumb, HSAPs are generally very stable as colloids when $\zeta > +25$ mV or $\zeta < -25$ mV. The PAC-AuNR-HSAPs created with either 20, 30, or 50 mg of HSA had zeta potential values of $\zeta = -38 \pm 1$, -42 ± 3 or -45 ± 3 mV, respectively, showing highly stable particle formations.

Aside from EPR effects mentioned previously, studies have shown that albumin-bound paclitaxel binds to the gp60 HSA receptor on the cell surface, facilitating transcytosis via the formation of caveolae; thus causing increased uptake of PAC into diseased cells.[39] Our formation of biofriendly particles are not only efficiently sized for EPR effects, but they also have the potential to mitigate damage to healthy cell membranes caused by toxic CTAB-coated AuNRs.[40] Since any residual CTAB is hidden by the HSAP shell, the toxicity caused by CTAB should be reduced.

3.2. Loading Efficiency of PAC into HSAPs and AuNR-HSAPs. The aim of this project was to create PAC-AuNR-HSAP composite particles for potential future use in PPTT. Because gold is readily coordinated by sulfur-containing moieties in the albumin (resulting in Au-albumin thiol bonds), we, and other researchers, have previously seen that the albumin coats the surface of the gold.[40,41] This protein corona layer results in the gold particles, which act as nuclei during coacervation of the AuNR-HSAPs.

To test whether the presence of AuNRs hindered the drug encapsulation ability of the HSAPs, 0.5 mg of PAC was added to separate particle batches consisting of either 30 mg of HSA or 30 mg of HSA and 1.5 mL of AuNRs solution. It was found that the PAC-HSAPs and the PAC-AuNR-HSAPs entrapped an average of 63.3 ± 14 and 91.8 ± 9 μg of PAC, respectively. There was a 45% increase in PAC loading when AuNRs were present in the particles. This was a surprising result and it is not fully known what caused this increase in PAC loading when AuNRs were present. We speculate that the PAC could have adsorbed onto the AuNRs because of a hydrophobic interaction with the trace CTAB present prior to and during the formation of the HSA corona layer.

Previous research has shown that the ammonium group of one CTAB binds to the surface of the gold and the hydrocarbon chain can interact with another CTAB hydrocarbon chain to form a bilayer. The second CTAB ammonium group is positively charged and free to bind to HSA. The hydrophobic pocket created in between the two CTAB molecules is free to bind drug. The amphiphilic properties of the HSA packing around the gold may have then reinforced the PAC placement.[9]

To find the loading efficiency of the paclitaxel in the PAC-AuNR-HSAPs, the preparation procedure in section 3.2 was followed with two distinct experimental changes: (1) the mass of HSA remained the same and the mass of PAC was varied and (2) the mass of HSA was varied and the mass of PAC remained constant. Figure 2a shows the results when 30 mg of HSA were prepared with either: 0.1, 0.25, or 0.5 mg of PAC. The resulting PAC-AuNR-HSAPs were successfully loaded with 17 ± 2, 39 ± 5, and 92 ± 14 μg of PAC, respectively. The particles created with 0.5 mg of PAC contained over 3 μg of drug per mg of HSA in finished particles.

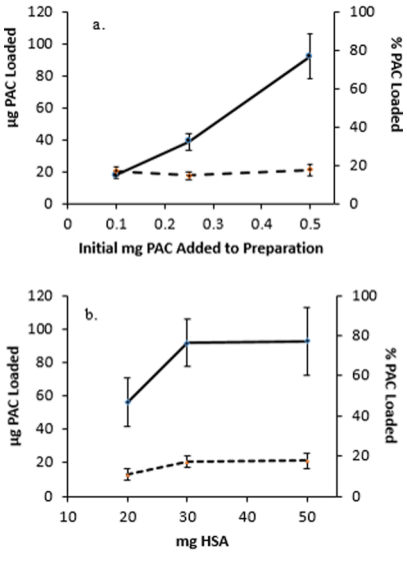

Figure 2. (a) (solid line) Micrograms of PAC loaded into the PAC-AuNR-HSAPs versus the milligrams of PAC initially added to the preparation vial and (dashed line) the percentage of loaded PAC vs PAC added to the preparation solution. (b) (solid line) Micrograms of PAC loaded into the PAC-AuNR-HSAPs vs the milligrams of HSA present in the preparation vial and (dashed line) the percentage of loaded PAC vs amount of HSA used.

DOI: 10.1021/acsami.5b00858
ACS Appl. Mater. Interfaces 2015, 7, 7101−7111

Since the final particle suspension was in a volume of 1 mL, the resulting concentration of drug in the suspension was 133 μM. This concentration is the amount of drug entrapped within the batch of particles and can potentially be released to the tumor site via PPTT and temporally during dynamic enzymatic activity in vivo. That loading concentration far exceeds the in vitro cytotoxicity of a paclitaxel-filled lipid emulsion in a previous study, which was shown to have a paclitaxel IC_{50} value of 5.5 μM on HeLa cells.[42] The IC_{50} value is the half-maximum inhibitory concentration, which is determined by a dose–response curve, and it indicates the concentration of drug that is required for 50% inhibition of the cancer cells in vitro.[43]

Figure 2b shows results when 0.5 mg of PAC was added to particle preparation batches containing either 20, 30, or 50 mg HSA. The resulting drug loading was 56.1 ± 14, 91.8 ± 14, and 92.7 ± 20 μg PAC, respectively. There was a larger increase in drug loading when increasing mass of HSA in the sample from 20 to 30 mg HSA; followed by a plateau in PAC loading when using 30 or 50 mg of HSA. The 30 mg of HSA sample was still able to hold the most drug per milligram of HSA: 3 μg PAC/mg HSA. The percent PAC loading data shown in Figures 2a and 2b confirm the particles do not entrap more than roughly 17% of the 0.5 mg of PAC added to the preparation solution even when more HSA is available. This result was not fully understood, except for the hypothesis that the cross-linking of these particles might be playing a role in the effective drug entrapment as both the 30 and 50 mg particle batches were theoretically cross-linked at 40%.

In short, when the amount of PAC introduced in the preparation process was increased, there was an increase in PAC loading into the particles. When AuNRs were present within the particles, the drug loading further increased. This drug payload increase is an achievement directly caused by this particular hybrid formulation. When the amount of HSA was increased, there was also an increase in drug-loading. Under the conditions used, we were successful in loading a sufficient amount of drug capable of killing the cancer cells: 91.8 ± 9 μg of PAC per mL of finished PAC-AuNR-HSAPs particle solution (133 μM).[42]

3.3. Effect of Cross-Linking on Drug Loading. The amine groups on the HSA are cross-linked by a condensation reaction with the aldehyde groups of glutaraldehyde.[35] It has been calculated that the lowest required amount of glutaraldehyde needed to quantitatively cross-link all 59 ε-amino groups present in 100 mg of HSA is approximately 58.8 μL (4.7×10^{-5} moles) of 8% (V/V) glutaraldehyde in H_2O.[35] All theoretical cross-linking calculations were based on this previous work, and it has been customary for groups working with this desolvation and cross-linking process to use percentage values to indicate the expected degree of cross-linking.[44]

To test whether the cross-linking played a major role in drug loading, two sample preparations of PAC-AuNR-HSAPs were created with 30 mg of HSA and 0.5 mg of PAC; one batch was theoretically cross-linked at 20% (2.87×10^{-6} moles glutaraldehyde) and the other at 40% (5.73×10^{-6} moles glutaraldehyde). As shown in Figure 3, the 40% cross-linked PAC-AuNR-HSAPs had more drug loaded (92 ± 14 μg) with less deviation, while the 20% cross-linked particles had less consistent drug loading (53 ± 49 μg). Although, some batches of the 20% cross-linked particles were capable of loading up to 102 μg of PAC, there was a large error associated with the loading. Therefore, cross-linking definitely plays a role in keeping the paclitaxel locked into the particles until it is provoked for release.

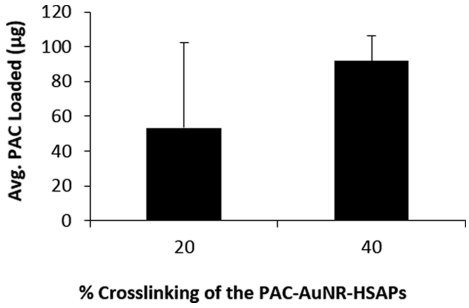

Figure 3. Average micrograms of PAC loaded into PAC-AuNR-HSAPs vs the percent of theoretical cross-linking of the particles. Error bars represent standard deviations of measurements ($n > 3$).

3.4. PAC-AuNR-HSAP and AuNR-HSAP Heating Capabilities. It has previously been discovered that when AuNR induced PPTT is used to create hyperthermia in human prostate tumor bearing mice, maintaining temperatures of 42–43 °C for 10 min showed an increase of macromolecular delivery into the tumor site.[45] In a separate study, when using paclitaxel-conjugated 11-mercaptoundecanoic acid-linked polyethylene glycol coated AuNRs, a combination of the drug and heating to 58 °C left absolutely no viable A549 breast cancer cells.[9] Our approach allows for heating via selective temperature ranges, depending on the dosage of the PAC-AuNR-HSAPs delivered and the NIR treatment time.

A cell well-plate was placed under the vertically mounted laser and particle batches suspended in water and ethanol were placed in the wells. The 808 nm laser was turned on at 2 W of power for up to 15 min while a thermocouple, placed on the side of the well, recorded the temperature continuously. The particle solution was then collected via a pipet, centrifuged and the supernatant was saved for drug content analysis. Figure 4 shows the heating trend (solid line) for PAC-AuNR-HSAPs created with 30 mg of HSA, 1.5 mL of AuNR stock, and 0.5 mg of PAC. The particles experience a sharp increase to 43 °C in roughly 5 min and continued to heat to 46° within 15 min. The dashed line in Figure 4 represents the heating of PAC-HSAPs with no AuNRs inside; it is shown that these particles never reached a temperature over normal body temperature. The graph clearly shows that the AuNRs are necessary to cause substantial heating. Consequently, only cells with HASP-AuNR and exposure to laser radiation would experience hyperthermia.

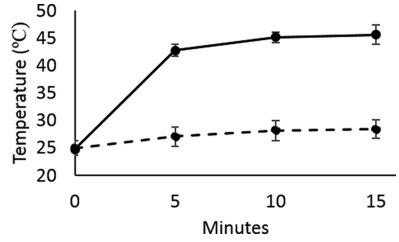

Figure 4. Heating trend in °C of (solid line) PAC-AuNR-HSAPs and (dashed line) PAC-HSAPs.

3.5. Drug Release via Photothermal Irradiation. Literature reports state that paclitaxel has cytotoxic activity at concentrations as low as 50 nM, and it was evident that the PAC-AuNR-HSAP delivery system was capable of loading far

DOI: 10.1021/acsami.5b00858
ACS Appl. Mater. Interfaces 2015, 7, 7101–7111

more paclitaxel than that (up to 133 μM in a 1 mL sample, shown in section 3.2), while still maintaining heating abilities.[46] The PAC-AuNR-HSAPs created in this work are true hybrids, where the anticancer functions of PPTT aided-uptake, heat ablation, EPR and drug release coexist, so it was important to know the heat-induced drug release. Our method must prove drug release of at least the minimum cytotoxic dose via PPTT and temporal release in order to be a viable treatment vehicle

In this study, the PAC-AuNR-HSAPs initially created with 0.1, 0.25, or 0.5 mg of PAC (created with 30 mg of HSA and cross-linked 40%) were irradiated with 808 nm NIR light for 15 min to monitor PAC release. These particles contained on average 56.1 ± 14, 91.8 ± 14, and 92.7 ± 20 μg of PAC and after only 15 min, they released 189 ± 108, 111 ± 33, and 124 ± 70 ng, respectively.

In each case, a slight burst of release less than 1% of the loaded PAC was shown. Although a small percentage, the induced release would be considered an effective dose, with the lowest average concentration of 145 nM released into the 1 mL of irradiated solution. This is actually a desirable outcome, as a quick complete release of the drug payload can result in lower antitumor efficacy due to the subsequently quick drug clearance from the body.[21] The ideal antitumor treatment would be to harness the initial shock of the heat ablation and paclitaxel dose in a localized area, followed by the slower, continued release of the drug penetrating further into the tumor site via the leaky vasculature and heightened metabolism of the site.

It is also worth noting that the particles which were created with different cross-linking percentages showed differences in drug release as well. The PAC-AuNR-HSAPs created with 20% theoretical cross-linking released over 4% of the entrapped drug; an average of 932 ng of PAC released vs 124 ng (less than 1%) released by the 40% cross-linked particles. As found with the loading, there is a large statistical error for the drug release associated with the lesser cross-linked particles: 932 ± 646 ng. The amount of drug that remains in the less tightly locked particles has a better chance of being released. Conversely, greater cross-linking allows for increased loading and the opportunity for prolonged release as well as decreased chances of drug release in areas other than the tumor site. These release results were compared to two control scenarios, where release was tested on irradiated PAC-HSAPs containing drug, but no AuNRs and on PAC-AuNR-HSAPs which were not irradiated. In both cases, the drug in the measured particle supernatant was below the detection limit of 10 ng of PAC/mL using HPLC analysis.

3.6. Temporal Drug Release. To show that the paclitaxel was indeed released continually from the PAC-AuNR-HSAPs after the initial irradiation period, three separate batches of PAC-AuNR-HSAPs samples (batches A, B, and C) were created (each with 0.5 mg of PAC and 40% cross-linking preparation parameters) and irradiated for 15 min. For each batch, the sample suspensions were centrifuged and the supernatants were removed for initial, laser provoked drug release analysis. Just as in section 3.5, the initial burst of drug release for each sample batch was below 1% of the total loaded drug.

The particle batches were then stored at 4 °C for a certain amount of time: batch A was stored for 7 days, batch B for 14 days and batch C for 21 days to monitor subsequent drug release when no further irradiation was performed past the initial laser session. Figure 5 shows the release trend for the postirradiated particles. Total drug released after 7, 14, and 21

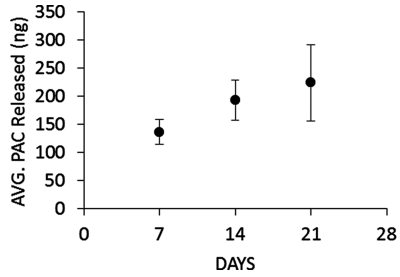

Figure 5. Average nanograms of PAC released vs time after a single 15 min laser treatment on day 0. Error bars represent standard deviation (n > 3).

days was 136 ± 22, 193 ± 36, and 224 ± 68 ng, respectively, for batches A, B, and C.

For example, this means that after 7 days, samples in batch A experienced a further drug release of 136 ± 22 ng in addition to the initial drug release the samples had already experienced during the irradiation session. Therefore, Figure 5 is not a cumulative representation of drug release including the irradiation-provoked release, but rather it is a representation of how the PAC-AuNR-HSAPs are capable of extended drug release after an initial PPTT treatment.

This release was in water at a low temperature without irradiation, so it should be noted that the dynamic activity of a tumor at normal body temperature and a slightly acidic pH (as seen in tumor sites) will enhance the release rate, especially if proteolytic enzymes are active.

Even though PAC-HSAPs with no gold nanorods inside did not experience an initial irradiation-provoked burst of drug release because of their inability to sufficiently heat, the PAC-HSAPs did release 104 ± 22 ng over a 7 day period, compared to 136 ± 22 for PAC-AuNR-HSAPs. This confirms that any particles which do not end up with a gold nanorod inside will still complete the function of controlled drug release over time.

Figure 6 shows the effect of irradiation time of nanograms of PAC release of particles created with 30 mg of HSA and 0.5 mg

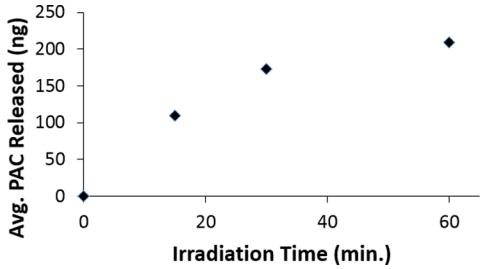

Figure 6. Effect of irradiation time on nanograms of PAC released. Particles created with 30 mg of of HSA and 0.5 mg of PAC.

PAC, with data measurements taken from a single experimental batch. There is a clear trend of drug release, indicating that the initial amount of drug released can be controlled and that there is a difference of release between nonirradiated samples and irradiated samples. The majority of the irraditation experiments were performed using only 15 min irradiation times, in order to keep the single-use laser therapy application time optimally minimal. More experiments on drug release vs irradiation time would need to be performed to obtain further statistical information, if desired. Experiments regarding multiple laser irradiation treatments over time could also be performed during in vivo research.

DOI: 10.1021/acsami.5b00858
ACS Appl. Mater. Interfaces 2015, 7, 7101−7111

Table 1. Effects of 15 min Irradiation, HSAP, PAC, and AuNR Combinations/Treatments on 4T1 Breast Cancer Cell Viability; Using 10, 20, or 30 μg PAC/mL of Total Treatment Solution and 9.5×10^{10}, 1.92×10^{11}, or 2.88×10^{11} AuNRs/mL of Total Treatment Solution[a]

	10 μg/mL PAC 9.5×10^{10} AuNRs/mL		20 μg/mL PAC 1.92×10^{11} AuNRs/mL		30 μg/mL PAC 2.88×10^{11} AuNRs/mL	
	irradiation	no irradiation	irradiation	no irradiation	irradiation	no irradiation
	% Cell Viability					
control		100.0 ± 1.2		100.0 ± 0.5		100.0 ± 0.6
HSAPs	99.6 ± 1.3	99.3 ± 1.6	99.5 ± 1.1	97.8 ± 0.5	95.1 ± 0.6	95.8 ± 0.5
PAC	46.1 ± 1.4	46.3 ± 1.5	28.9 ± 0.3	31.5 ± 0.6	19.5 ± 0.7	22.6 ± 0.5
PAC-HSAPs	74.8 ± 1.7	73.1 ± 1.1	62.0 ± 0.6	59.8 ± 1.4	38.0 ± 1.1	40.7 ± 1.6
AuNRs	44.7 ± 0.8	49.9 ± 0.8	26.6 ± 0.4	39.3 ± 0.5	9.0 ± 0.8	20.2 ± 1.8
AuNR-HSAPs	71.6 ± 1.0	96.7 ± 1.2	51.7 ± 0.9	92.9 ± 1.0	46.7 ± 0.6	91.2 ± 2.5
PAC-AuNR-HSAPs	57.3 ± 0.9	70.4 ± 1.0	21.5 ± 0.3	34.7 ± 0.3	6.4 ± 0.4	17.6 ± 0.6
laser	99.5 ± 1.4	99.2 ± 1.1	99.1 ± 0.5	99.5 ± 0.6	98.4 ± 0.7	99.8 ± 0.5

[a]The control cells were not subject to irradiation. For cells undergoing the laser treatment, the "no irradiation" experimental condition indicates the cells were placed under the laser, but kept in dark conditions. All sample irradiations were performed with a single 15 min exposure at 808 nm (2 mW laser). $N = 3$ for each treatment.

However, what makes this preliminary PAC released vs irradiation time result even more promising is that PAC-HSAPs without AuNRs inside would travel alongside the PAC-AuNR-HSAPs in vivo and they may still experience the heating effects of the neighboring gold-filled particles. So, under biological conditions, the PAC-HSAPs may still experience the initial burst of drug release during irradiation, as well as undergo their temporal chemotherapeutic function.

3.7. 4T1 Breast Cancer Cells Photothermal and Chemotherapeutic in Vitro Studies. Treated and untreated 4T1 breast cancer cells were compare the effects of the various treatments, each studied with and without irradiation: no particles (control), unloaded HSAPs, free paclitaxel in ethanol, PAC-HSAPs, free AuNRs, AuNR-HSAPs, and PAC-AuNR-HSAPs. For the cells experiencing one of the aforementioned treatments, an aliquot of the PAC, AuNR or various particle solutions was added to the 4T1 cells and laser irradiations were done 2−3 min after the treatment additions (for those samples requiring NIR). The cells were allowed to incubate for 24 h. After incubation, an MTT assay was performed to measure cell vialibity; the results are shown in Table 1.

As seen in Table 1, the untreated control cells and the laser treated blank cells remained nearly 100% viable with or without irradiation; indicating that the 808 nm near-infrared light was harmless to the cells with the duration used. The cells treated with the unloaded HSAPs also remained 95−99% viable under irradiated and dark conditions. This high viability proves that the protein particle is not harmful to the breast cancer cells and is a good candidate for a chemotherapuetic and photothermally active particle carrier. Not surprisingly, the free PAC caused more than half of the cells to die at the lower dose of paclitaxel. The extent of necrosis increased with increasing paclitaxel dose. For these studies, the PAC was delivered in an ethanol solvent vehicle. This vehicle likely enhanced PAC uptake since its aqueous solubility is very low. It is notable that the laser irradiation caused a slight increase in cell death from 22.6 ± 0.5% to 19.5 ± 0.7% ($p < 0.05$) when the cells were treated with paclitaxel alone at 30 μg of PAC/mL. This corroborates with previous studies that have shown an increase in drug uptake with the utilization of NIR light.[7,29]

It was also unremarkable that the free AuNRs caused a dramatic drop in cell viability, which was most likely due to the trace CTAB (toxic to cells) present in the AuNR solution. Laser irradiation of cells containing AuNRs showed estensive, dose-dependent cell death, presumably because of cell heating. When used in the highest concentration of 2.88×10^{11} AuNRs/mL, the nanorods had the greatest laser-induced cell death effects on the cells.

When the nanorods were covered in the spherical HSAP shell to create AuNR-HSAPs, the HSA acted as a protective barrier for the cells against the harmful effects of the free AuNRs (again, presumably because of CTAB on their surface). This result is demonstrated by the fact that with equal numbers of AuNRs present, cell viability remained above 91% when the AuNRs were encapsulated in HSAPs with no irradiation applied. This protection phenomenon is critical in preventing damage to healthy cells. While encapsulation of the AuNRs into the HSAPs eliminated direct toxicity, encapsulation did not hinder the heating ability of the nanorods. When the AuNR-HSAPs were irradiated, they were substantially more effective at facilitating cell death than the nonirratiated AuNR-HSAPs ($p < 0.001$). When compared to the irradiated PAC-AuNR-HSAPs, the irradiated AuNR-HSAPs still did not cause as much cell death ($p < 0.05$) as the drug-gold-protein hybrid particles. The fact that the AuNR-HSAP treatment only exhibited meaningful cell death with irradiation clearly demonstrates that the particles can be selectively activated to kill only cells in the targeted treatment area, thereby protecting nontargeted cells from damage.

In section 3.1, Figure 1c demonstrates that not every HSAP contained a AuNR inside. Therefore, we needed an understanding of the effects of PAC-HSAPs that were loaded with only drug in order to determine what would happen to particles that traveled to the tumor site along with the PAC-AuNR-HSAPs. Since our particles are similar to Abraxane (with a differing preparation method and final concentration), it was assumed that the PAC-HSAPs would cause a significant amount of cell death. Table 1 clearly shows that the PAC-HSAPs were able to facilitate cell death: from about 40.7 to 73.1% cell viability was observed, depending on encapsulated PAC concentration, without irradiation. When laser irradiation was introduced, the viability range shifted only very slightly from 38.0 to 74.8%. Since the cells were allowed to sit with the PAC-HSAPs for 24 h, the drug release can be considered dynamic and enzymatic when compared to study in section 3.5, where paclitaxel release was negligible (at least under 10 ng PAC/mL) when unprovoked.

DOI: 10.1021/acsami.5b00858
ACS Appl. Mater. Interfaces 2015, 7, 7101−7111

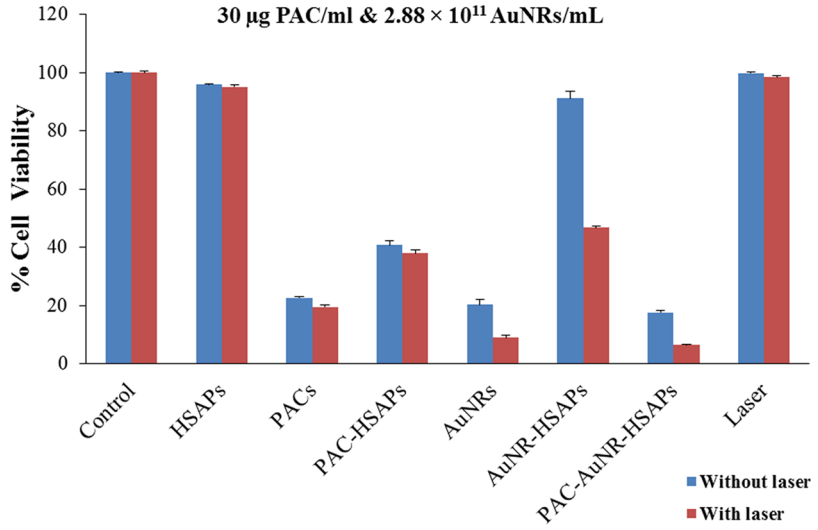

Figure 7. Comparison of all irradiated and nonirradiated treatment types on 4T1 breast cancer cell viability after treatment; using 30 mg HSAPs, 30 μg/mL of paclitaxel and 2.88 × 10^{11} AuNRs/mL when present in the treatment formulation. All treatments (N = 3) compared to PAC-AuNR-HSAPs were statistically different (p < 0.001) for irradiated and nonirradiated treatments; except for AuNR-HSAPs which were statistically different (p < 0.05).

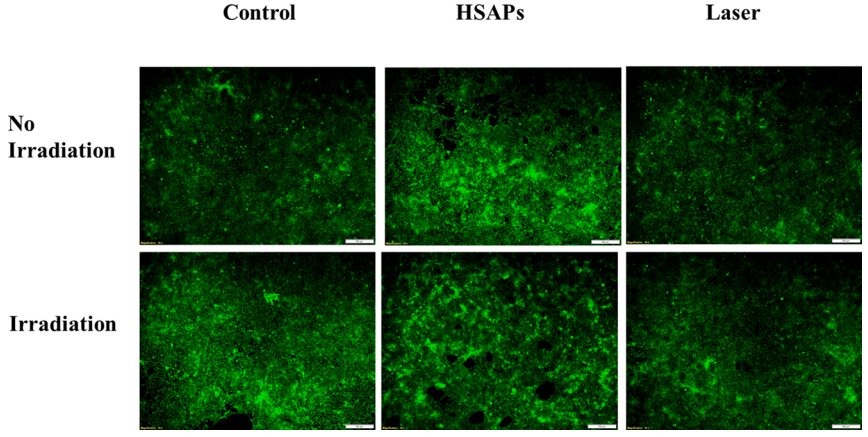

Figure 8. Fluorescence microscopy images of the cytotoxic effects on 4T1 breast cancer control cells and cells treated with unloaded HSAPs or the NIR laser. (White scale bar denotes 100 μm).

In section 3.6 it was shown that the particles underwent a temporal drug release over a 7 day period when dispersed in water; releasing 104 ± 22 ng, an amount more than sufficient for cell necrosis. The in vitro treatment involved only a 24 h incubation period before the MTT assay, but under dynamic cell conditions, it is assumed that complete drug release would take place faster due to proteoloytic destruction of the HSAPs within the cells.

Table 1 and Figure 7 show the impressive cancer cell-killing abilities of the composite PAC-AuNR-HSAP treatment vehicle. The irradiated PAC-AuNR-HSAPs caused more cell necrosis than PAC-HSAPs across all paclitaxel concentrations, with or without irradiation (p < 0.001). When the photothermally active material was not heat-activated, the PAC-AuNR-HSAPs still showed more cell death than the drug-loaded particles (p < 0.05 for 10 and 20 μg PAC/mL sample encapsulated treatments; p < 0.001 for 30 μg PAC/mL sample encapsulated treatments).

There are three theories for this increase in cell death: (1) as the cells break down the PAC-AuNR-HSAPs in the lysosomes through enzymatic activity, the AuNRs are translocated into the mitochondria, thus causing an intracellular pathway for toxicity, (2) the CTAB is exposed via the particle breakdown causing the increase in toxicity, or (3) the particle size difference plays an important role. The PAC-AuNR-HSAPs had an average particle size of 299 ± 6 and the PAC-HSAPs were 158 ± 7 nm; possibly causing the larger particles to undergo phagocytosis, while the smaller particles underwent pinocytosis; resulting in different particle-cell interactions within the 24 h period.[47,48] More studies are needed to pinpoint the cause of increased cell death affected by PAC-AuNR-HSAPs vs PAC-HSAPs when no irradiation was performed.

When irradiation was performed on the PAC-AuNR-HSAPs, there was a noticeable difference between the cell viability of the gold and drug loaded particles versus the PAC-HSAPs (Figure 7) (p < 0.001). When using 30 μg/mL PAC and 2.88 × 10^{11} AuNRs/mL in an aliquot of the PAC-AuNR-HSAPs, nearly all of the cells were killed, with only 6.4% of the cells remaining alive in the treated well after 24 h. Since we have concluded that the entirety of the encapsulated drug is not released after the initial 15 min irradiation session, it is expected

DOI: 10.1021/acsami.5b00858
ACS Appl. Mater. Interfaces 2015, 7, 7101−7111

that the cell viability will decrease further due to temporal drug release and additional irradiation sessions.

The PAC-AuNR-HSAPs had the best overall treatment outcome, even when compared to the free paclitaxel and free AuNRs. For the highest dose (30 μg/mL PAC, 2.88 × 10^{11} AuNR/mL), cell viability decreased from 17.6% to 6.4% when irradiation was added ($p < 0.05$), indicating that the addition of near-infrared radiation improved the treatment effectiveness. Similar enhancements were observed for the other doses studied. Overall, the combination of PAC-AuNR-HSAPs with irradiation, was the most effective of all treatments studied (at least $p < 0.05$).

Based on the data provided in Table 1, we made a preliminary estimate of IC50 values and provided those in Supporting Information (Table S1).

3.8. Microscopy of 4T1 Breast Cancer Cells Treatment Studies. Fluorescence microscopy was performed with a 10× magnification on the control and treated 4T1 breast cancer cells to confirm the results of the MTT assay. Figures 8−10 show the treatment effects with and without irradiation using 20 μg/mL paclitaxel and 1.92 × 10^{11} AuNRs/mL, if present in the treatment formulation.

The cells were treated in the same manner as the cells in section 3.7, however the imaged cells were treated with acridine orange, which fluoresces at ∼525 nm when bound to DNA. The images validate the cell viability data obtained via the MTT assay. Figure 8 displays the findings that the control, HSAPs treated and laser treated cells maintain healthy DNA function 24 h after treatment.

Figure 9 shows the patchiness of the fluorescence in the plane of view, which is an indication of the breakdown of DNA

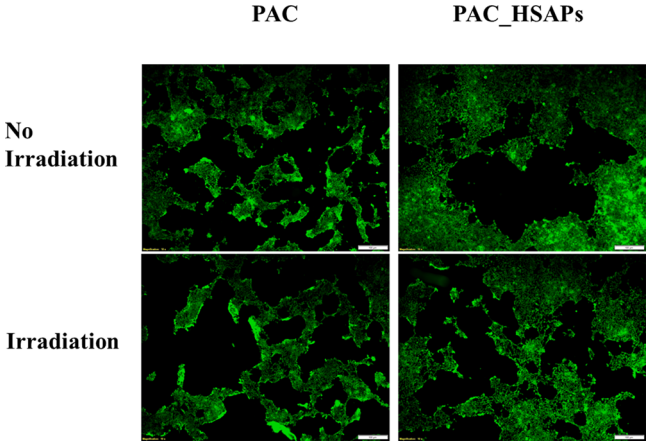

Figure 9. Fluorescence microscopy images of the cytotoxic effects on 4T1 breast cancer cells when treated with free paclitaxel (20 μg PAC/mL) or PAC-HSAPs (20 μg PAC/mL). (White scale bar denotes 100 μm).

in the 4T1 cells when PAC was introduced in the treatment formulations. Since paclitaxel is a mitotic inhibitor, it has detrimental effects on DNA formation and repair within the cancer cells. For the PAC and PAC-HSAP treatments, no substantial differences were observed between fluorescence microscope images of irradiated and nonirradiated samples.

Figure 10 further illustrates the effects of the DNA destruction within the cancer cells when the AuNRs were added as part of the treatment combinations. The free AuNRs caused significant cellular breakdown and necrosis without irradiation. These effects are most likely due to the presence of toxic CTAB on the surface of the AuNRs. With irradiation, cell death was substantially enhanced as the result of plasmonic heating of the AuNRs. When AuNRs were encapsulated in HSAPs, toxicity was dramatically improved as evident from the fluorescence microscopy image. The HSAP particles themselves pose little toxicity, and the AuNRs are sufficiently encapsulated to eliminate their toxic effects. Addition of NIR radiation of the AuNR-HSAP treated cells resulted in substantial cell death due to hyperthermia as seen by the decreased fluorescence in Figure 10.

It is important to note that NIR heating of gold nanorods for in vivo photothermal therapy may require active targeting for certain cancers to be most effective as sufficient collective photothermal conversion is needed to reach adequate cell hyperthermic temperatures.[49] The tissue margin which experiences residual heating must be taken into account to avoid an adverse increase in temperature of the surrounding, healthy extra-tumoral area. Effective penetration of NIR to the tumor site is also necessary for effective treatment.

Overall, the composite PAC-AuNR-HSAPs showed the best results for cancer cell death. Without heating the particles via NIR irradiation, the PAC loaded particles caused impressive cell death after 24 h. When the photothermally active gold within the PAC-AuNR-HSAPs were activated with 808 nm radiation, the PAC-AuNR-HSAPs became extremely effective at killing the cells as clearly noted in the minimal fluorescence in Figure 10 for this treatment. As mentioned previously, the fact that these particles will accumulate in tumors and that their effectiveness is greatest when irradiated indicates that targeted killing of cancer cells is possible with this treatment.

The PAC-AuNR-HSAPs showed more visible cell death than any other treatment combination; even more than the treatments with free PAC and the irradiated AuNRs. The combination of the drug and the photothermal therapy within the treatment vehicle clearly cause an increase in necrosis with much less inherent toxicity, because of the protecting value of the HSA (as evidenced by the lack of cell death caused when no drug is present in the HSAPs and non-irradiated AuNR-HSAPs).

4. CONCLUSIONS

In this study, hybrid PAC-AuNR-HSAPs were successfully prepared with simultaneously loaded drug and encapsulated AuNRs to show that these composite particles can serve as platforms for preparing new drug therapies. The combined approach will allow killing of cancer cells by both hyperthermia and localized chemotherapy treatment and is more likely to eliminate all cancer cells. Cells with resistance to heat will be killed by PAC, and cells that are resistant to PAC will be killed by hyperthermia, dramatically decreasing the chance of survival for drug or thermally resistant cells. The photothermal approach not only results in hyperthermic treatment, but it also serves as a trigger for drug release once the particles have reached their targeted tissue and may aid in controlled release only at the tumor site.

When compared to free drug, free AuNRs, AuNR-HSAPs, and PAC-HSAPs, the combination platform of irradiated, drug and gold-loaded PAC-AuNR-HSAPs performed the best in 4T1 breast cancer cell in vitro studies. Fluorescence microscopy images of the treated breast cancer cells further solidified the findings that the multifunctional particles were more effective at causing cancer cell death. These particles are capable of housing

DOI: 10.1021/acsami.5b00858
ACS Appl. Mater. Interfaces 2015, 7, 7101−7111

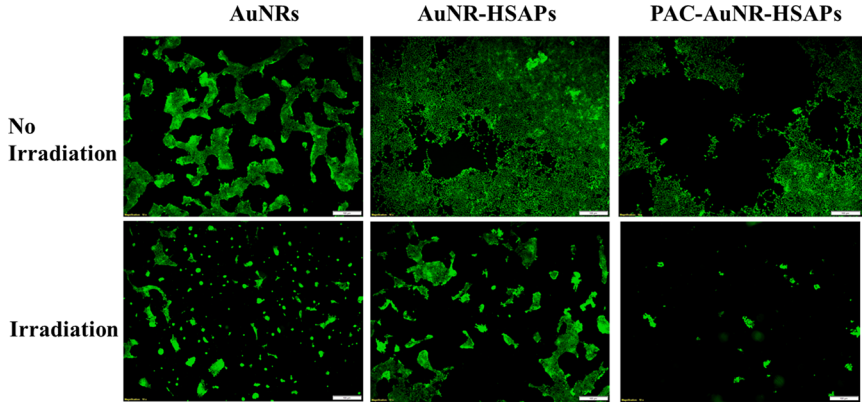

Figure 10. Fluorescence microscopy images of the cytotoxic effects on 4T1 breast cancer cells when treated with free AuNRs (1.92×10^{11} AuNRs/mL), AuNR-HSAPs (1.92×10^{11} AuNRs/mL) or PAC-AuNR-HSAPs (20 μg PAC/mL and 1.92×10^{11} AuNRs/mL). (White scale bar denotes 100 μm).

more than one drug simultaneously along with the AuNRs; making a tailor-made treatment regime a potential future possibility for a patient's quality of life. Functionalizing the surface of the HSAPs with disease-specific targeting ligands may lead to even more effective delivery of cancer therapies to the site of the disease, boosting effectiveness and reducing damage to healthy tissue.[49]

■ ASSOCIATED CONTENT

Supporting Information

Estimated IC_{50} values based on a linear regression of cell viability versus dose for three levels of drug and three levels of nanoparticle dosing. This material is available free of charge via the Internet at http://pubs.acs.org.

■ AUTHOR INFORMATION

Corresponding Author

*E-mail: mtarr@uno.edu.

Notes

The authors declare no competing financial interest.

■ ACKNOWLEDGMENTS

This work was supported by the Louisiana Board of Regents under grant LEQSF (2007-12)-ENH-PKSFI-PRS-04, by The National Institute of Health under grants CA089121 and AI103106, and by the University of New Orleans Office of Research and Sponsored Programs.

■ REFERENCES

(1) Choi, W.; Kim, J.; Kang, C.; Byeon, C.; Kim, Y.; Tae, G. Tumor Regression In Vivo by Photothermal Therapy Based on Gold-Nanorod-Loaded, Functional Nanocarriers. *ACS Nano* **2011**, *5*, 1995−2003.

(2) Cole, J.; Mirin, N.; Knight, M.; Goodrich, G.; Halas, N. Photothermal Efficiencies of Nanoshells and Nanorods for Clinical Therapeutic Applications. *J. Phys. Chem. C* **2009**, *113*, 12090−12094.

(3) Jang, B.; Park, J.; Tung, C.; Kim, I.; Choi, Y. Gold Nanorod-Photosensitizer Complex for Near-Infrared Fluorescence Imaging and Photodynamic/Photothermal Therapy in vivo. *ACS Nano* **2011**, *5*, 1086−1094.

(4) Terentyuk, G.; Ivanov, A.; Polyanskaya, N.; Maksimova, I.; Skaptsov, A.; Chumakov, D.; Khlebtsov, B.; Khlebtsov, N. Photothermal Effects Induced by Laser Heating of Gold Nanorods in Suspensions and Inoculated Tumours During in Vivo Experiments. *Quantum Electron.* **2012**, *42*, 380−389.

(5) Huschka, R.; Zuloaga, J.; Knight, M.; Brown, L.; Nordlander, P.; Halas, N. Light-Induced Release of DNA from Gold Nanoparticles: Nanoshells and Nanorods. *J. Am. Chem. Soc.* **2011**, *133*, 12247−12255.

(6) Alkilany, A.; Thompson, L.; Boulos, S.; Sisco, P.; Murphy, C. Gold Nanorods: Their Potential for Photothermal Therapeutics and Drug Delivery, Tempered by the Complexity of their Biological Interactions. *Adv. Drug Delivery Rev.* **2012**, *64*, 190−199.

(7) van der Zee, J. Heating the Patient: A Promising Approach? *Ann. Oncol.* **2002**, *13*, 1173−1184.

(8) Gormley, A.; Larson, N.; Banisadr, A.; Robinson, R.; Frazier, N.; Ray, A.; Ghandehari, H. Plasmonic Photothermal Therapy Increases the Tumor Mass Penetration of HPMA Copolymers. *J. Controlled Release* **2013**, *166*, 130−138.

(9) Ren, F.; Bhana, S.; Norman, D. D.; Johnson, J.; Xu, L.; Baker, D.; Parrill, A.; Huang, X. Gold Nanorods Carrying Paclitaxel for Photothermal-Chemotherapy of Cancer. *Bioconjugate Chem.* **2013**, *24*, 376−386.

(10) Charan, S.; Sanjiv, K.; Singh, N.; Chien, F.; Chen, Y.; Nergui, N.; Huang, S.; Kuo, C.; Lee, T.; Chen, P. Development of Chitosan Oligosaccharide-Modified Gold Nanorods for in Vivo Targeted Delivery and Noninvasive Imaging by NIR Irradiation. *Bioconjugate Chem.* **2012**, *23*, 2173−2182.

(11) Peralta, D.; Wheeler, D.; Zhang, J.; Tarr, M. Encapsulating Gold Nanomaterials into Size-Controlled Human Serum Albumin Nanoparticles for Cancer Therapy Platforms. *J. Microencapsulation* **2014**, *31*, 824−831.

(12) Fasano, M.; Curry, S.; Terreno, E.; Galliano, M.; Fanali, G.; Narciso, P.; Notari, S.; Ascenzi, P. The Extraordinary Ligand Binding Properties of Human Serum Albumin. *IUBMB Life* **2005**, *57*, 787−796.

(13) Fanali, G.; di Masi, A.; Trezza, V.; Marino, M.; Fasano, M.; Ascenzi, P. Human Serum Albumin: From Bench to Bedside. *Mol. Aspects Med.* **2012**, *33*, 209−290.

(14) Ulbrich, K.; Michaelis, M.; Rothweiler, F.; Knobloch, T.; Sithisarn, P.; Cinatl, J.; Kreuter, J. Interaction of Folate-Conjugated Human Serum Albumin (HSA) Nanoparticles with Tumour Cells. *Int. J. Pharm.* **2011**, *406*, 128−134.

(15) Jithan, A.; Madhavi, K.; Madhavi, M.; Prabhakar, K. Preparation and Characterization of Albumin Nanoparticles Encapsulating Curcumin Intended for the Treatment of Breast Cancer. *Int. J. Pharm. Invest.* **2011**, *1*, 119−125.

(16) von Storp, B.; Engel, A.; Boeker, A.; Ploeger, M.; Langer, K. Albumin Nanoparticles with Predictable Size by Desolvation Procedure. *J. Microencapsulation* **2012**, *29*, 138−146.

(17) Wagner, S.; Rothweiler, F.; Anhorn, M. G.; Sauer, D.; Riemann, I.; Weiss, E. C.; Katsen-Globa, A.; Michaelis, M.; Cinatl, J., Jr; Schwartz, D.; Kreuter, J.; von Briesen, H.; Langer, K. Enhanced Drug Targeting by Attachment of an Anti αv Integrin Antibody to

DOI: 10.1021/acsami.5b00858
ACS Appl. Mater. Interfaces 2015, 7, 7101−7111

Doxorubicin Loaded Human Serum Albumin Nanoparticles. *Biomaterials* **2010**, *31*, 2388−2398.
(18) Kim, T.; Jiang, H.; Youn, Y.; Park, C.; Lim, S.; Jin, C.; Tak, K.; Lee, H.; Lee, K. Preparation and Characterization of Apo2L/TNF-related Apoptosis-inducing Ligand-loaded Human Serum Albumin Nanoparticles with Improved Stability and Tumor Distribution. *J. Pharm. Sci.* **2011**, *100*, 482−491.
(19) Kim, T.; Jiang, H.; Youn, Y.; Park, C.; Tak, K.; Lee, S.; Kim, H.; Jon, S.; Chen, X.; Lee, K. Preparation and Characterization of Water-Soluble Albumin-Bound Curcumin Nanoparticles with Improved Antitumor Activity. *Int. J. Pharm.* **2011**, *403*, 285−291.
(20) Surapaneni, M.; Das, S.; Das, N. Designing Paclitaxel Drug Delivery Systems Aimed at Improved Patient Outcomes: Current Status and Challenges. *ISRN Pharmacol.* **2012**, *2012*, No. 623139.
(21) Zhang, J.; He, B.; Qu, W.; Cui, Z.; Wang, Y.; Zhang, H.; Wang, J.; Zhang, Q. Preparation of the Albumin Nanoparticle System Loaded with Both Paclitaxel and Sorafenib and its Evaluation in vitro and in vivo. *J. Microencapsulation* **2011**, *28*, 528−536.
(22) Montana, M.; Verhaeghe, P.; Terme, T.; Vanelle, P.; Rathelot, P. Albumin-Bound Paclitaxel: The Benefit of This New Formulation in the Treatment of Various Cancers. *J. Chemother.* **2011**, *23*, 59−66.
(23) Yardley, D. A. nab-Paclitaxel Mechanisms of Action and Delivery. *J. Controlled Release* **2013**, *170*, 365−72.
(24) Portal, A.; Pernot, S.; Siauve, N.; Landi, B.; Lepere, C.; Colussi, O.; Rougier, P.; Zaanan, A.; Verriere, B.; Taieb, J. Sustained Response with Gemcitabine Plus nab-Paclitaxel After Folfirinox Failure in Metastatic Pancreatic Cancer: Report of an Effective New Strategy. *Clin. Res. Hepatol. Gastroenterol.* **2014**, *38*, 23−26.
(25) Von Hoff, D.; Ramanathan, R.; Borad, M.; Laheru, D.; Smith, L.; Wood, T.; Korn, R.; Desai, N.; Trieu, V.; Iglesias, J.; Zhang, H.; Soon-Shiong, P.; Shi, T.; Rajeshkumar, N.; Maitra, A.; Hidalgo, M. Gemcitabine Plus nab-Paclitaxel is an Active Regimen in Patients with Advanced Pancreatic Cancer: A Phase I/II Trial. *J. Clin. Oncol.* **2011**, *29*, 4548−4554.
(26) Von Hoff, D.; Ervin, T.; Arena, F.; Chiorean, E.; Infante, J.; Moore, M.; Seay, T.; Tjulandin, S.; Ma, W.; Saleh, M.; Harris, M.; Reni, M.; Dowden, S.; Laheru, D.; Bahary, N.; Ramanathan, R.; Tabernero, J.; Hidalgo, M.; Goldstein, D.; Van Cutsem, E.; Wei, X.; Iglesias, J.; Renschler, M. Increased Survival in Pancreatic Cancer with nab-Paclitaxel Plus Gemcitabine. *New Engl. J. Med.* **2013**, *369*, 1691−1703.
(27) Anhorn, M.; Wagner, S.; Kreuter, J.; Langer, K.; von Briesen, H. Specific Targeting of HER2 Overexpressing Breast Cancer Cells with Doxorubicin-Loaded Trastuzumab-Modified Human Serum Albumin Nanoparticles. *Bioconjugate Chem.* **2008**, *19*, 2321−2331.
(28) Sebak, S.; Mirzaei, M.; Malhotra, M.; Kulamarva, A. Human Serum Albumin Nanoparticles as an Efficient Noscapine Drug Delivery System for Potential use in Breast Cancer: Preparation and in Vitro Analysis. *Int. J. Nanomed.* **2010**, 525−532.
(29) Kroeze, S.; van Melick, H.; Nijkamp, M.; Kruse, F.; Kruijssen, L.; van Diest, P.; Bosch, J.; Jans, J. Incomplete Thermal Ablation Stimulates Proliferation of Residual Renal Carcinoma Cells in a Translational Murine Model. *BJU International* **2012**, *110*, 281−286.
(30) Tang, H.; Kobayashi, H.; Niidome, Y.; Mori, T.; Katayama, Y.; Niidome, T. CW/Pulsed NIR Irradiation of Gold Nanorods: Effect on Transdermal Protein Delivery Mediated by Photothermal Ablation. *J. Controlled Release* **2013**, *171*, 178−183.
(31) Huang, X.; El-Sayed, I.; Qian, W.; El-Sayed, M. Cancer Cell Imaging and Photothermal Therapy in the Near-Infrared Region by Using Gold Nanorods. *J. Am. Chem. Soc.* **2006**, *128*, 2115−2120.
(32) Stone, J.; Jackson, S.; Wright, D. Biological Applications of Gold Nanorods. *Wiley Interdiscip. Rev. Nanomed. Nanobiotechnol.* **2011**, *3*, 100−109.
(33) Warner, S. Diagnostics Plus Therapy = Theranostics. *Scientist* **2004**, *18*, 38−39.
(34) Weber, C.; Kreuter, J.; Langer, K. Desolvation Process and Surface Characteristics of HSA Nanoparticles. *Int. J. Pharm.* **2000**, *196*, 197−200.
(35) Langer, K.; Anhorn, M.; Steinhauser, I.; Dreis, S.; Celebi, D.; Schrickel, N.; Faust, S.; Vogel, V. Human Serum Albumin (HSA) Nanoparticles: Reproducibility of Preparation Process and Kinetics of Enzymatic Degradation. *Int. J. Pharm.* **2008**, *347*, 109−117.
(36) Mehravar, R.; Jahanshah, M.; Sagatoleslami, N. Fabrication and Evaluation of Human Serum Albumin (HSA) Nanoparticles for Drug Delivery Application. *Int. J. Nanosci.* **2009**, *8*, 319−322.
(37) Lin, W.; Coombes, A.; Davies, M.; Schacht, E.; Davis, S.; IIIum, L. Preparation of sub-100 nm Human Serum Albumin Nanospheres Using a pH-Coacervation Method. *J. Drug Targeting* **1993**, *1*, 237−243.
(38) Wyatt-Technology. *Wyatt Technology Corporation Handbook*; Wyatt Technology Corporation: Santa Barbara, CA, 2011.
(39) Paal, K.; Muller, J.; Hegedus, L. High Affinity Binding of Paclitaxel to Human Serum Albumin. *Eur. J. Biochem.* **2001**, *268*, 2187−2191.
(40) Wang, L.; Li, J.; Pan, J.; Jiang, X.; Ji, Y.; Li, Y.; Qu, Y.; Zhao, Y.; Wu, X.; Chen, C. Revealing the Binding Structure of the Protein Corona on Gold Nanorods Using Synchrotron Radiation-Based Techniques: Understanding the Reduced Damage in Cell Membranes. *J. Am. Chem. Soc.* **2013**, *135*, 17359−17368.
(41) Yoshimura, K.; Uemura, H. Role of Vaccine Therapy for Renal Cell Carcinoma in the Era of Targeted Therapy. *Int. J. Urology* **2013**, *20*, 744−755.
(42) Lundberg, B.; Risovic, V.; Ramaswamy, M.; Wasan, K. A Lipophilic Paclitaxel Derivative Incorporated in a Lipid Emulsion for Parenteral Administration. *J. Controlled Release* **2003**, *86*, 93−100.
(43) Sebaugh, J. Guidelines for Accurate EC_{50}/IC_{50} Estimation. *Pharm. Stat.* **2011**, *10*, 128−134.
(44) Wacker, M.; Zensi, A.; Kufleitner, J.; Ruff, A.; Schutz, J.; Stockburger, T.; Marstaller, T.; Vogel, V. A Toolbox for the Upscaling of Ethanolic Human Serum Albumin (HSA) Desolvation. *Int. J. Pharm.* **2011**, *414*, 225−232.
(45) Modabber, M.; Martin, J.; Athreya, S. Thermal Versus Impedance-Based Ablation of Renal Cell Carcinoma: A Meta-analysis. *Cardiovasc. Intervention Radiol.* **2014**, *37*, 176−185.
(46) Kim, S.; Yu, J.; Lee, J.; Park, E.; Chi, S. Sensitive HPLC Method for Quantitation of Paclitaxel (Genexol in Biological Samples with Application to Preclinical Pharmacokinetics and Biodistribution. *J. Pharm. Biomed. Anal.* **2005**, *39*, 170−176.
(47) Chithrani, B.; Ghazani, A.; Chan, W. Determining the Size and Shape Dependence of Gold Nanoparticle Uptake into Mammalian Cells. *Nano Lett.* **2006**, *6*, 662−668.
(48) Wang, L.; Liu, Y.; Li, W.; Jiang, X.; Ji, Y.; Wu, X.; Xu, L.; Qiu, Y.; Zhao, K.; Wei, T.; Li, Y.; Zhao, Y.; Chen, C. Selective Targeting of Gold Nanorods at the Mitochondria of Cancer Cells: Implications for Cancer Therapy. *Nano Lett.* **2011**, *11*, 772−780.
(49) Alkilany, A.; Murphy, C. Toxicity and Cellular Uptake of Gold Nanoparticles: What We Have Learned So Far? *J. Nanopart. Res.* **2010**, *12*, 2313−2333.

DOI: 10.1021/acsami.5b00858
ACS Appl. Mater. Interfaces 2015, 7, 7101−7111